MOLECULAR IMAGING AND BIOLOGY

Molecular Imaging and Biology
DOI 10.1007/s11307-021-01639-4

WMIS World Molecular Imaging Society

esmi european society for molecular imaging

Check for updates

RESEARCH ARTICLE

Longitudinal FRET Imaging of Glucose and Lactate Dynamics and Response to Therapy in Breast Cancer Cells

Jianchen Yang[1], Tessa Davis[1], Anum S. Kazerouni[1], Yuan-I. Chen[1], Meghan J. Bloom[1], Hsin-Chih Yeh[1,2], Thomas E. Yankeelov[1,3,4,5,6,7], and John Virostko[3,4,6]

1Department of Biomedical Engineering, The University of Texas At Austin, Austin, TX 78712, USA
[2]Texas Materials Institute, The University of Texas At Austin, Austin, TX 78712, USA
[3]Department of Diagnostic Medicine, The University of Texas At Austin, 201 E. 24th Street, 1 University Station (C0200), Austin, TX 78712, USA
[4]Department of Oncology, The University of Texas At Austin, Austin, TX 78712, USA
[5]Oden Institute for Computational Engineering and Sciences, The University of Texas At Austin, Austin, TX 78712, USA
[6]Livestrong Cancer Institutes, The University of Texas At Austin, Austin, TX 78712, USA
[7]Department of Imaging Physics, The University of Texas MD Anderson Cancer Center, Houston, TX 77030, USA 2021

Abstract

Purpose: The reprogramming of cellular metabolism is a hallmark of cancer. The ability to noninvasively assay glucose and lactate concentrations in cancer cells would improve our understanding of the dynamic changes in metabolic activity accompanying tumor initiation, progression, and response to therapy. Unfortunately, common approaches for measuring these nutrient levels are invasive or interrupt cell growth. This study transfected FRET reporters quantifying glucose and lactate concentration into breast cancer cell lines to study nutrient dynamics and response to therapy.

Procedures: Two FRET reporters, one assaying glucose concentration and one assaying lactate concentration, were stably transfected into the MDA-MB-231 breast cancer cell line. Correlation between FRET measurements and ligand concentration were measured using a confocal microscope and a cell imaging plate reader. Longitudinal changes in glucose and lactate concentration were measured in response to treatment with $CoCl_2$, cytochalasin B, and phloretin which, respectively, induce hypoxia, block glucose uptake, and block glucose and lactate transport.

Results: The FRET ratio from the glucose and lactate reporters increased with increasing concentration of the corresponding ligand ($p < 0.005$ and $p < 0.05$, respectively). The FRET ratio from both reporters was found to decrease over time for high initial concentrations of the ligand ($p < 0.01$). Significant differences in the FRET ratio corresponding to metabolic inhibition were found when cells were treated with glucose/lactate transporter inhibitors.

Conclusions: FRET reporters can track intracellular glucose and lactate dynamics in cancer cells, providing insight into tumor metabolism and response to therapy over time.

Key words Fluorescence · Time-resolved microscopy · MDA-MB-231 · Metabolism · Oncometabolite · Hypoxia · Warburg effect

Correspondence to: John Virostko*; e-mail: jack.virostko@austin.utexas.edu*

Introduction

Solid tumors are characterized by the presence of irregular vasculature [1], resulting in a spatially heterogeneous environment with both insufficient delivery of nutrients, such as glucose and oxygen, and reduced ability to remove metabolic wastes. To meet the high demand in energy production and biosynthesis in proliferating tumors, cancer cells adapt to the microenvironment with altered metabolism, which is one of the hallmarks of cancer [2]. Warburg [3, 4] discovered that in cancer cells glucose is converted to lactate with a high rate of glycolysis even in the presence of sufficient oxygen. Although not fully understood, it is thought that tumor cells are highly glycolytic to maintain rapid proliferation. While glycolysis is significantly less efficient in generating ATP compared to oxidative phosphorylation, it generates ATP at a faster rate [5, 6]. Furthermore, glycolysis functions as a carbon influx to provide materials for downstream biosynthesis [4, 7]. Following glycolysis, lactate is converted from pyruvate by lactate dehydrogenase (LDH) and creates an acidic environment favoring tumor cells over normal cells [8, 9]. The control of intracellular and extracellular acidity is associated with tumorigenesis, cancer progression, diffusion, invasion, and escape from immune destruction [10, 11]. Thus, glucose and lactate play important roles in driving tumor metabolism and progression.

The ability to measure glucose and lactate concentration would improve our understanding of cancer metabolism and guide development of new therapies targeting metabolic pathways. Glucose analogs with radioactive labels like 2-deoxy-2-[^{18}F]fluoro-D-glucose ([^{18}F]FDG) [12] or fluorescent labels like 2-(N-(7-nitrobenz-2-oxa-1,3-diazol-4-yl)Amino)-2-deoxyglucose (2-NBDG) [13] are used to study the kinetics of glucose uptake, but they inhibit glycolysis and block downstream reactions. Common approaches for measuring lactate are based on enzymatic reactions followed by photometric or amperometric procedures [14, 15]. These approaches are invasive as they require the consumption of substrate and/or the sample and require large quantities of cells. In the present work, we utilize two FRET (Förster or fluorescence resonance energy transfer) reporters for the measurement of glucose [16] and lactate [17] concentrations. Figure 1 illustrates the design of the glucose and lactate FRET reporters. The binding of the target molecules would lead to a conformational change that alters the distance/orientation between the coupled fluorescent proteins, resulting in an increase/decrease in FRET efficiency. Since their development, these reporters have been applied to study metabolic signaling and neuronal activity in astrocytes [18–22]. They also have been employed in breast cancer cells to study the role of carbonic anhydrase IX in hypoxia [23–25], the interaction between stromal and breast cancer cells [26, 27], bioenergetics and toxicity of mitochondria [28, 29], and intra-tumor heterogeneity of metabolic states [30]. Importantly, these previous studies employed measurements at a single time point or measurement of kinetics on a time scale of seconds to minutes. To the best of our knowledge, longer term monitoring of glucose and lactate dynamics in cancer cells has not been performed.

In this study, we constructed stably transfected glucose and lactate FRET reporters in the triple negative breast cancer cell line, MDA-MB-231. We established a standard curve for ligand concentration–dependent FRET ratio response at a single time point and measured the longitudinal FRET ratio change when the cells were supplied with different glucose or lactate concentrations. We then perturbed the cellular glucose and lactate concentrations by introducing a hypoxia inducer or inhibitors of glucose or lactate transport. We found that FRET reporters can be used to track changes in glucose and/or lactate concentration over time and detect dynamic changes in cancer cell metabolism in response to therapy.

Materials and Methods

Cell Culture and Transfection

The triple negative breast cancer cell line, MDA-MB-231, was obtained from the American Type Culture Collection (ATCC, Manassas, VA) and grown in high-glucose (25 mM) Dulbecco's Modified Eagle's Medium (DMEM, Thermo Fisher Scientific, Waltham, MA) containing 10 % fetal bovine

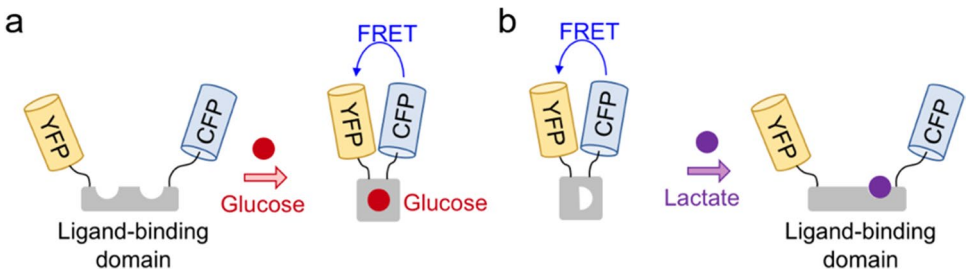

Fig. 1. Illustrations of the design of the glucose (**a**) and lactate (**b**) FRET reporters. The FRET reporters exploit the resonance energy transfer between a pair of fluorescent proteins, with a ligand-binding domain for the target molecule. The FRET efficiency depends on the distance and orientation between the fluorescent proteins. **a** The conformational change of the glucose reporter when bound to glucose leads to an increase in the FRET efficiency. **b** The conformational change of the lactate reporter when bound to lactate leads to a decrease in the FRET efficiency.

serum, 2 mM L-glutamine, and 100 units/ml penicillin–streptomycin at 37 °C/5 % CO_2.

The plasmid carrying the glucose FRET sensor, pcDNA3.1 FLII12Pglu-700uDelta6 (17,866, gift of Wolf Frommer [16]), and the plasmid carrying the lactate FRET sensor, Laconic/pcDNA3.1(-) (44,238, gift of Luis Felipe Barros [17]) were obtained from Addgene (Watertow, MA). Prior to transfection, MDA-MB-231 cells were seeded in a 6-well plate and allowed to achieve 70–80 % confluence. Transfection with plasmids containing either glucose or lactate FRET-based reporters was performed with Lipofectamine LTX & PLUS Reagent (Thermo Fisher Scientific, Waltham, MA) according to the manufacturer's instructions. Transfection medium (Opti-MEM I Reduced-Serum Medium, Thermo Fisher Scientific, Waltham, MA) contained no serum or antibiotics. Six hours post-transfection, the transfection medium was replaced with DMEM culture medium. Three days post-transfection, selection was initiated using DMEM containing 100 μg/mL G418 (Sigma-Aldrich, St. Louis, MO). After 2 weeks of selection, the cells were resuspended in medium at 1×10^6 cells/ml and sorted with a BD FACSAria flow cytometer (BD Biosciences, San Jose, CA). The sorting was based on YFP (yellow fluorescent protein) emission where untransfected cells were used as negative control. Sorted cells expressing the FRET reporters were collected and re-cultured for subsequent studies.

Measurement of Glucose and Lactate from Extracted FRET Reporters

Prior to protein extraction, MDA-MB-231 cells transfected with either the glucose or lactate FRET reporter were seeded in a T-175 flask and allowed to achieve 80–90 % confluence. The Halt Protease and Phosphatase Inhibitor Cocktail (Thermo Fisher Scientific, Waltham, MA) was added to the cell lysis reagent CelLytic M (Sigma-Aldrich, St. Louis, MO) in a 1:100 ratio. Whole-cell proteins containing the glucose or lactate reporter were extracted with cell lysis reagent according to the manufacturer's instructions.

The solution of whole-cell protein extraction containing the glucose or lactate reporter was added to a 96-well black plate and diluted in phosphate buffered saline (PBS, Caisson Labs, Smithfield, UT) to glucose or lactate concentrations of 0, 0.1, 0.2, 0.5, 0.8, 1, 2, 5, 8, or 10 mM. PBS with the same glucose or lactate concentration was added to the same 96-well plate as a control group. Fluorescence was measured with a BioTek Cytation 5 Cell Imaging Multi-Mode Reader (BioTek Instruments, Inc., Winooski, VT) at 37 °C/5 % CO_2. The proteins were excited at a wavelength of 433 nm, and fluorescence emissions of CFP (cyan fluorescent protein) and YFP were measured at a wavelength of 485 nm and 528 nm. The ratio between the emissions was used to characterize the reporters. For glucose, the FRET ratio was defined as the fluorescence intensity at 528 nm divided by the intensity at 485 nm. For lactate, the FRET ratio was defined as the fluorescence intensity at 485 nm divided by the intensity at 528 nm, due to differences in the construction of the glucose and lactate reporters. More specifically, the binding of glucose reduces the distance between the donor and the acceptor, leading to an increase in energy transfer, while the binding of lactate increases the distance between the donor and the acceptor, reducing the energy transfer. Measurements were performed on at least three independent protein extracts. The standard deviation was calculated from 3 measurements. The values from the control group were quantified to determine background noise and subtracted from the values of the wells containing the FRET reporters.

Measurement of Glucose and Lactate in Intact Cells

Twenty-four hours prior to imaging, MDA-MB-231 cells transfected with either glucose or lactate FRET reporter were seeded in an 8-well chamber slide and allowed to achieve 30–40 % confluence. The cells were placed in glucose-free medium for 30 min before adding glucose to the cell culture to achieve final concentrations of 0, 0.5, 1.0, 2.0, 5.0, 10.0, or 15.0 mM. The images were scanned three times with dwell time 0.1 ms/pixel before and after the addition of glucose by ISS Alba v5 Laser Scanning Confocal Microscope (ISS, Inc., Champaign, IL). The images were taken by the 405-nm laser light focused through a 20× objective (UPLSAPO, Olympus) and the fluorescence CFP and YFP were detected by two avalanche photodiodes (SPCM-AQR-15, Perkin Elmer) after passing the bandpass filters (445/40, 585/40 nm, Semrock), respectively.

Imaging was also performed using a BioTek Cytation 5 Cell Imaging Multi-Mode Reader. Twenty-four hours prior to imaging, MDA-MB-231 cells expressing either the glucose or lactate FRET reporter were seeded in a 96-well black plate and allowed to achieve 30–40 % confluence. Cell culture medium was changed to DMEM with different glucose or lactate concentrations (0, 0.1, 0.2, 0.5, 0.8, 1, 2, 5, 8, or 10 mM) and incubated at 37 °C for 10 min. Images were captured with a CFP (excitation wavelength 445 nm, emission wavelength 510 nm) filter cube and a CFP-YFP-FRET V2 (excitation wavelength 400 nm, emission wavelength 550 nm) filter cube. For longitudinal experiments, images were collected at 0, 1, 2, 3, 6, 9, and 12 h after media change. The standard deviation was calculated from 24 images.

FRET Image Processing

Image preprocessing was performed using Gen5 Software on the plate reader (BioTek Instruments, Inc., Winooski, VT). An automatic background flattening with default parameters was applied to images from CFP channel and CFP-YFP-FRET channel with the background set to "dark." All subsequent image processing was performed in Matlab (The Mathworks,

Inc., Natick, MA). First, a k-means clustering approach was applied on the CFP channel images using the Matlab function "kmeans" to segment cells expressing the FRET reporter [31]. The resultant mask was applied to the images from both the CFP channel and CFP-YFP-FRET channel. For the glucose reporter, the FRET ratio at each pixel was calculated by dividing the signal intensities from the masked CFP-YFP-FRET images over the signal intensities from the masked CFP images, as is commonly done for the quantification of FRET reporters [16]. For the lactate measurements, the signal intensities from the masked CFP images were divided by the signal intensities from the masked CFP-YFP-FRET images. Pixels with FRET ratios greater than 97.5 % or lower than 2.5 % of the population distribution were considered outliers and excluded from analysis. The FRET ratio for each image was calculated as the average of all non-zero pixel-wise FRET ratios.

For all experiments, the mean and the standard deviation of FRET ratios of all the images collected were calculated. Values greater than or smaller than two times the standard deviation from the mean value were considered outliers and removed [32]. Additionally, for experiments with multiple timepoint measurements, the mean and the standard deviation of FRET ratios of all the images from all time points were calculated and values greater than or smaller than two times the standard deviation from the mean value were considered outliers and removed.

To account for inter-assay differences in FRET measurements, quantification of FRET was expressed as a normalized ratio relative to a measurement made in the absence of ligand (0 mM glucose or lactate). The normalized ratio was calculated from the function: $r_{norm} = r / r_{lf}$, where r is the measured FRET ratio and r_{lf} is the ligand-free FRET ratio. The FRET measurements were fit to a single site-binding isotherm:

$$S = (r - rlf)/(rsa - rlf) = [ligand]/(Ka + [ligand]) \quad (1)$$

where S is the saturated-binding portion; $[ligand]$ is the ligand (glucose or lactate) concentration; r is the FRET ratio at the prescribed concentration; r_{lf} is the ligand-free FRET ratio; r_{sat} is the FRET ratio at saturation; and K_a is the binding affinity between the ligand and the reporter [16]. Fitting the data to Eq. (1) was performed in Matlab with the least square optimization algorithm "lsqcurvefit" to minimize the residual sum of squares.

Longitudinal Imaging of Glucose and Lactate in Response to Therapy

Following characterization and validation of glucose and lactate measurements using FRET reporters, we then employed them to image treatment response. Figure 2 illustrates the pathways and interventions involved in this treatment study. All imaging of therapeutic response was performed using a BioTek Cytation 5 Cell Imaging Multi-Mode Reader at 37 °C/5 % CO_2. Twenty-four hours prior to imaging, MDA-MB-231 cells transfected with the FRET reporter were seeded in a 96-well black plate and allowed to achieve 30–40 % confluence. We introduced $CoCl_2$ to induce hypoxia and inhibit oxidative phosphorylation [33] in MDA-MB-231 cells transfected with the lactate FRET reporter. The medium was changed to DMEM with 5 mM glucose and $CoCl_2$ of different concentrations (0, 50, 100, 200, and 500 μM). Images were acquired at 0, 6, 12, 24, 36, 48, and 60 h after addition of $CoCl_2$. To inhibit glucose uptake by tumor cells via glucose uptake transporters (GLUT) [34], we employed cytochalasin B (a GLUT1 inhibitor) [20, 35, 36]. MDA-MB-231 cells transfected with the glucose and lactate FRET reporters were incubated in DMEM with 5 mM glucose and cytochalasin B at concentrations of 0, 1, 2, and 4 μM. Images were acquired at 0, 24, and 60 h. Finally, we perturbed lactate export via monocarboxylic transporter (MCT) inhibition [37, 38] using phloretin, which is both a GLUT1 and MCT4 inhibitor [17, 39]. MDA-MB-231 cells transfected with the glucose and lactate FRET reporters were incubated in DMEM with 5 mM glucose and phloretin concentrations of 0, 10, and 20 μM. Images were acquired at 0, 24, and 60 h. The standard deviation was calculated from 48 images at each time point.

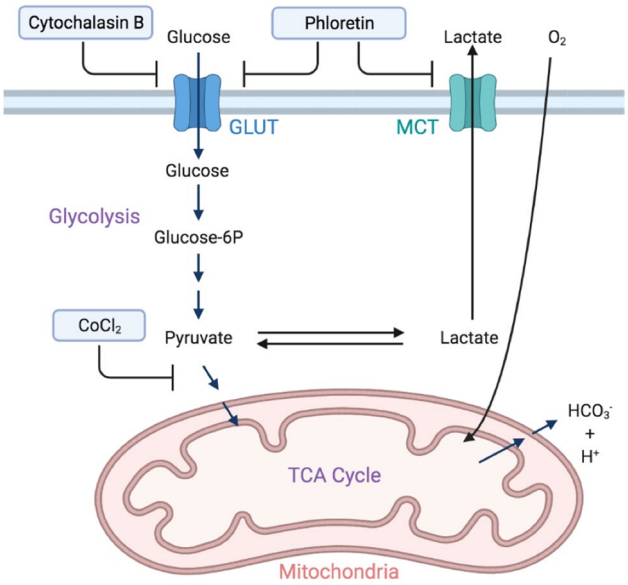

Fig. 2. Illustration of cell metabolism pathways and targets of nutrient perturbation assayed in this study. Interventions to alter metabolism (shown in blue boxes) were cytochalasin B, which inhibits GLUT1; phloretin, which inhibits GLUT1 and MCT4; and $CoCl_2$, which inhibits oxidative phosphorylation. GLUT, glucose transporter; MCT, monocarboxylic transporter; TCA cycle, tricarboxylic acid cycle.

Statistical Analysis

All statistical analysis was performed with Matlab. The Z-test was used to determine significant differences in FRET ratio change before and after addition of glucose. Spearman's

rank correlation coefficient (ρ) was used for comparison between FRET ratio and ligand concentration or time. One-way ANOVA and two-sample unpaired *t*-test were used to determine differences in FRET ratio in response to therapy. Differences were considered significant if $p < 0.05$.

Results

Generation and Characterization of MDA-MB-231 Cells with Glucose or Lactate Reporters

Stable transfection of MDA-MB-231 cells expressing either a glucose or lactate FRET reporter was generated by antibiotic selection followed by expression-based sorting with flow cytometry. When the cells were excited with the excitation wavelength for CFP, emission from both CFP and CFP-YFP-FRET channels (Fig. 3) was observed, demonstrating energy transfer from CFP to YFP in the presence of the corresponding ligand (glucose or lactate).

To characterize the function of the glucose FRET reporter, MDA-MB-231 cells stably expressing the glucose FRET reporter were imaged with a confocal microscope before and after the addition of glucose into glucose-free medium. The acquired images were processed to generate the masks labeling the fluorescent signals for CFPex/CFPem images (CFP-mask, Fig. 4a, c) and CFPex/YFPem images (YFP-mask, Fig. 4b and d), where the suffixes "ex" and "em" refer to excitation and emission, respectively. Imaging was performed before (Fig. 4a and b) and after the addition of glucose (Fig. 4c and d). The distribution of CFP emission (Fig. 4e) shifted to the left after addition of glucose (i.e., a lower intensity), while the distribution of YFP emission (Fig. 4f) slightly shifted to the right. The average CFP intensity decreased by 10.7 ± 0.6 % ($p < 0.0001$), while the average YFP increased by 6.2 ± 1.0 % ($p < 0.0001$), demonstrating an increased FRET ratio. The pixel-wised FRET ratio was calculated, and the distribution of the FRET ratio before and after the addition of glucose was compared. The distribution of the FRET ratio (Fig. 4g) shifted to the right after addition of glucose, reflecting an average FRET ratio increase of 22.5 ± 0.8 % ($p < 0.0001$). The FRET ratio normalized to the ratio of the cells in glucose-free medium increased with increasing glucose concentration (Fig. 4h; $\rho = 0.98$, $p < 0.0005$). The trend aligns well with our previous study [40].

Characterization of glucose or lactate FRET reporters was also performed using a cell plate reader equipped with a cell culture chamber to enable long-term imaging. The normalized FRET ratio of the solution containing the extracted glucose reporter was found to increase with increasing glucose concentration (Fig. 5a; $\rho = 0.96$, $p < 0.0001$). The normalized FRET ratio of the solution containing the extracted lactate reporter was also found to increase with increasing lactate concentration (Fig. 5b; $\rho = 0.96$, $p < 0.0001$). For intact cells, the normalized FRET ratio from cells expressing the glucose reporters increased with increasing glucose concentration (Fig. 5c; $\rho = 0.87$, $p < 0.0005$). Similarly, the normalized FRET ratio from cells stably expressing the lactate reporters also increased with increasing lactate concentration (Fig. 5d; $\rho = 0.69$, $p < 0.005$).

Longitudinal Dynamics of FRET Ratio with Different Initial Ligand Concentrations

We performed longitudinal imaging to determine how the FRET ratio changed over time as glucose and lactate

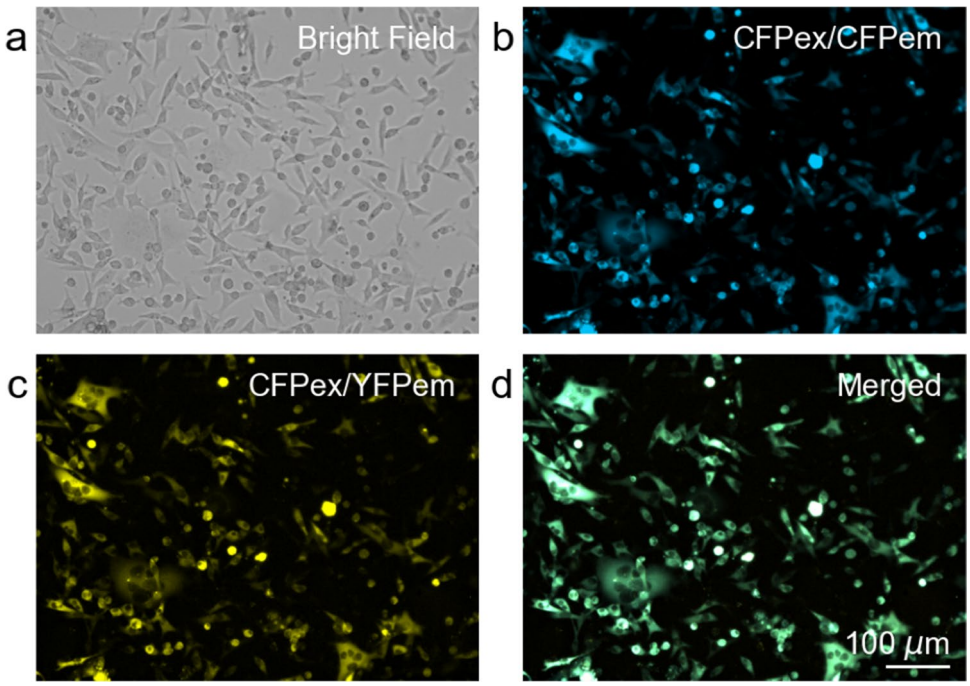

Fig. 3. Representative images of MDA-MB-231 cells constitutively expressing the glucose FRET reporter. **a** displays a bright field image. **b** displays a fluorescent image with excitation wavelength for CFP and emission wavelength for CFP, which detects the donor fluorophore of the FRET reporter. **c** displays a fluorescent image with excitation wavelength for CFP and emission wavelength for YFP, which detects the acceptor fluorophore of the FRET reporter. **d** displays the merged fluorescent signals from (**b**) and (**c**). The fluorescent signals co-localized in the cytoplasm from both CFP and CFP-YFP-FRET channels with an excitation wavelength for CFP demonstrated energy transfer from CFP to YFP.

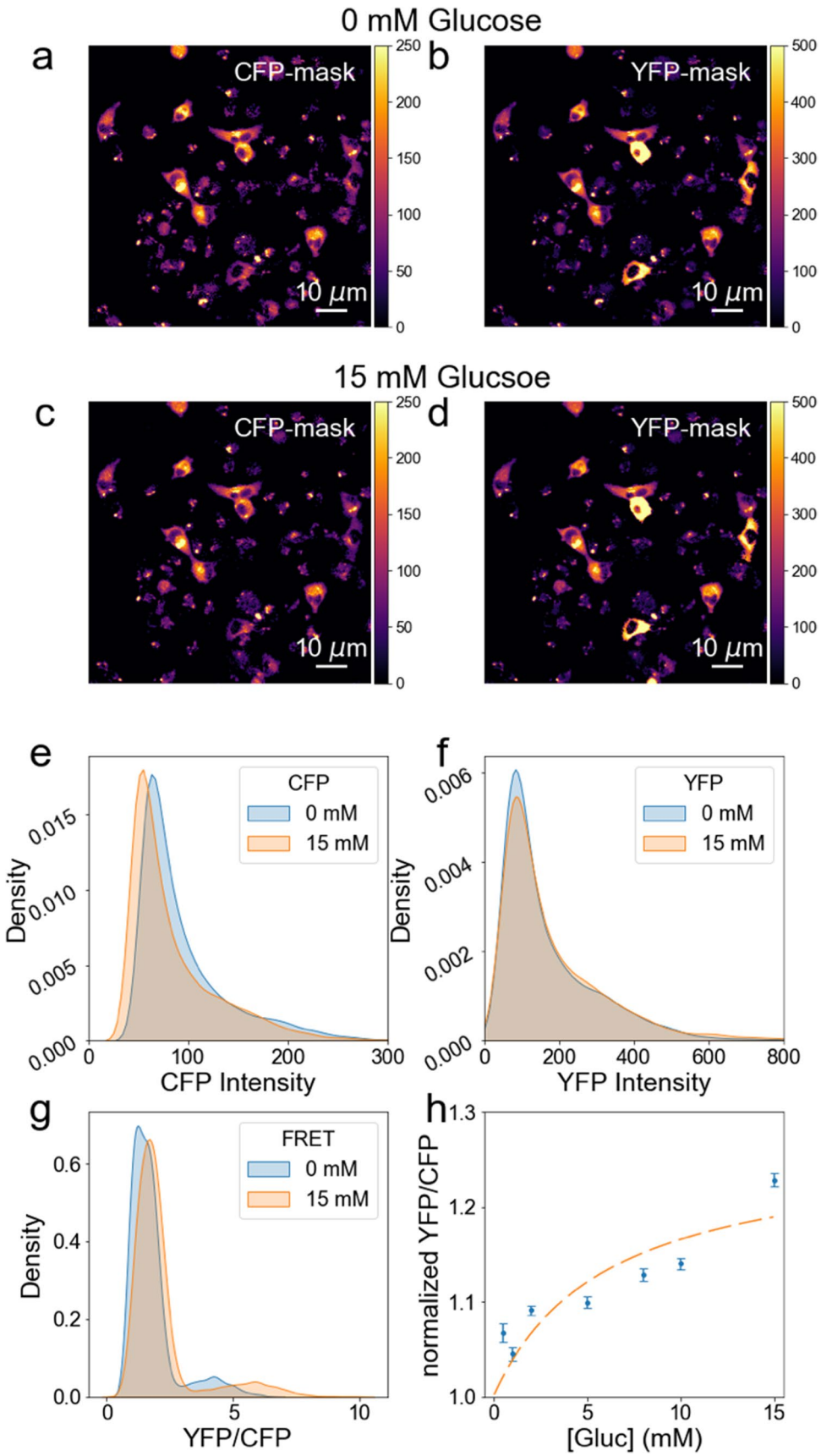

Fig. 4. FRET signals from the glucose reporter measured with a confocal microscope display response to glucose. **a** displays the mask of CFP emissions with 0 mM glucose. **b** displays the mask of YFP emissions with 0 mM glucose. (Note that the color map for (**a**) and (**b**) are different for better display.) **c** displays the mask of CFP emissions with 15 mM glucose. **d** displays the mask of YFP emissions with 15 mM glucose. **e** shows the distribution of CFP emission with 0 mM and 15 mM glucose. **f** shows the distribution of YFP emission with 0 mM and 15 mM glucose. **g** shows the distribution of pixel-wised FRET ratio with 0 mM and 15 mM glucose, indicating an increase in FRET measurement after the addition of glucose. **h** shows the relationship between average normalized FRET ratios and glucose concentration across a range of glucose values. The FRET ratio normalized to the ratio of cells in glucose-free medium increased with increasing glucose concentration. The normalized FRET ratios are shown in blue, while a curve fitting a single site-binding isotherm are displayed as an orange dashed line. The error bars indicate the standard deviation of the normalized FRET ratio calculated from each image.

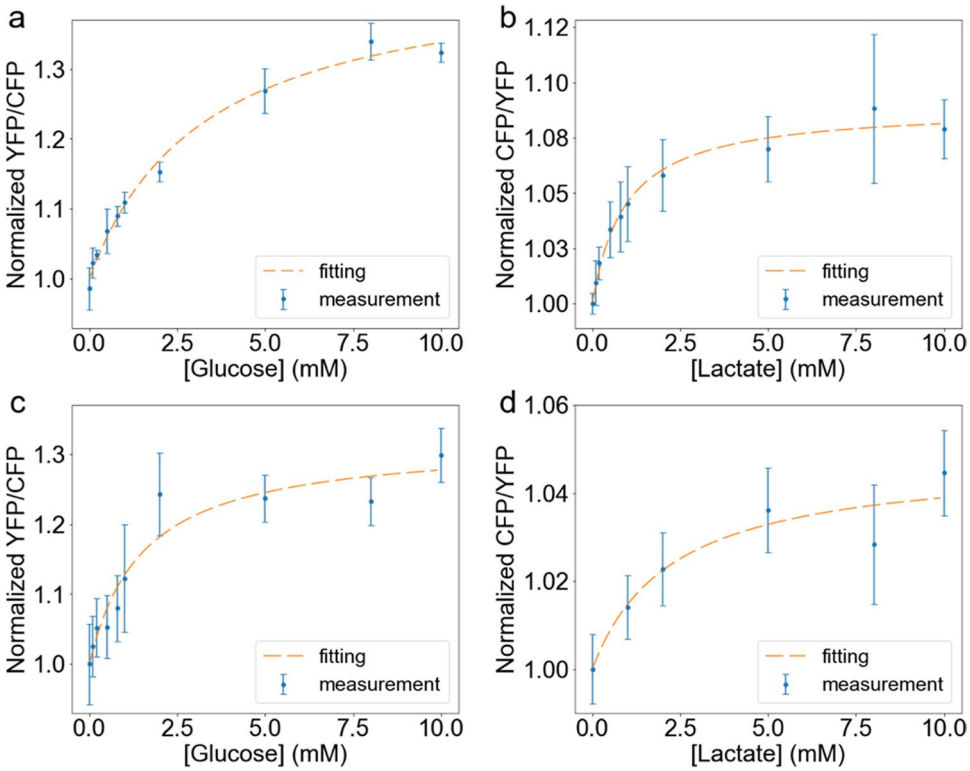

Fig. 5. The FRET ratios for both the glucose and lactate reporters are ligand concentration dependent as measured by plate reader. **a** shows the normalized FRET ratio from the solution of extracted whole-cell protein containing the glucose reporter. **b** shows the normalized FRET ratio from the solution of extracted whole-cell protein containing the lactate reporter. **c** shows the normalized FRET ratio from cells stably expressing the glucose reporter. **d** shows the normalized FRET ratio from cells stably expressing the lactate reporter. For each panel, the normalized FRET ratio and 95 % confidence interval are shown in blue, while curves fitting a single site-binding isotherm are displayed as an orange dashed line. Ligand concentrations can be estimated from the fitting curve with FRET ratio measured.

were consumed and produced by cellular metabolism. At each time point, the normalized FRET ratio from the cell line expressing the glucose reporter was found to increase with increasing glucose concentration (Fig. 6a; all $\rho > 0.81$, $p < 0.005$). The normalized FRET ratio for glucose was found to decline over time with significance for initial glucose concentration ≥ 2 mM ($p < 0.05$), while there was no significant change for initial glucose concentration below 2 mM. At each time point, the normalized FRET ratio from the cells stably expressing the lactate reporter was found to increase with increasing lactate concentration (Fig. 6b; $\rho > 0.85$, $p < 0.005$).

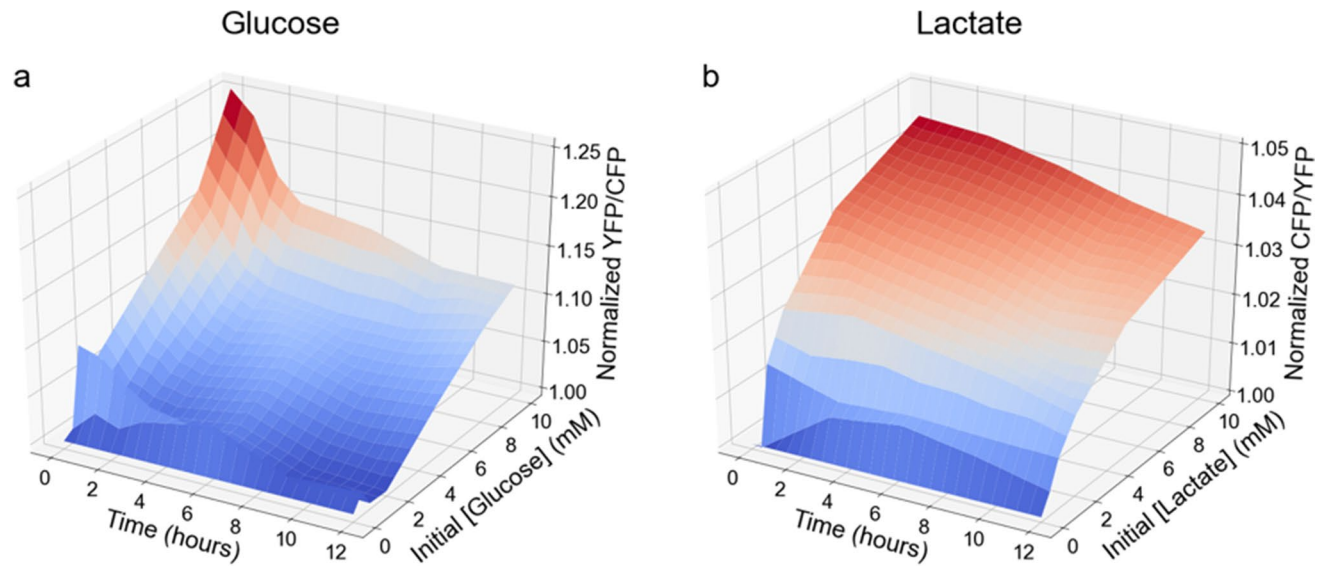

Fig. 6. Longitudinal FRET ratio measurements over 12 h with different initial concentrations of ligand. **a** shows the longitudinal FRET ratio change with different initial glucose levels. The normalized FRET ratio decreased over time corresponding to glucose consumption by the cells. At each time point, the normalized FRET ratio increased with increasing glucose concentration. **b** shows the longitudinal FRET ratio change with different initial lactate levels. The normalized FRET ratio decreased over time as lactate was consumed for initial lactate levels ≥ 2 mM. At each time point, the normalized FRET ratio increased with increasing lactate concentration.

For cells with initial lactate concentration of 10 mM, the normalized FRET ratio decreased over time ($p < 0.05$).

Measuring the Accumulation of Lactate Induced by Hypoxia

$CoCl_2$ is known to induce hypoxia and thus could lead to the accumulation of lactate as a result of enhanced glycolysis in the tumor cells. We imaged cells expressing the lactate FRET reporter over time to study the effect of $CoCl_2$ on the intracellular lactate level. At 6, 12, 36, 48, and 60 h, the normalized FRET ratio was found to increase with increasing $CoCl_2$ concentration (Fig. 7a; $\rho = 1.00$, $p < 0.05$). In particular, for cells treated with 500 μM $CoCl_2$, the normalized FRET ratio was found to increase over time ($\rho = 1.00$, $p < 0.005$). For cells treated with lower concentrations of $CoCl_2$, there were no significant correlations between the normalized FRET ratio and time. At baseline, there were no significant differences among the normalized FRET ratio of cells treated with different concentrations of $CoCl_2$. However, at 60 h, there was a significant difference ($p < 0.01$) between cells treated with 200 or 500 μM $CoCl_2$ and cells treated with lower concentrations, as well as between cells treated with 200 μM $CoCl_2$ and cells treated with 500 μM $CoCl_2$ (Fig. 7b; $p < 0.0001$).

Measuring the Effect of Nutrient Transporter Inhibitors on Glucose and Lactate Concentrations

Cytochalasin B is a GLUT inhibitor that inhibits glucose uptake but does not directly target lactate transport. We imaged cells expressing the glucose or lactate FRET reporter over time to study the effect of cytochalasin B on intracellular nutrient level. For the glucose reporter, immediately following addition of cytochalasin B, there was a significant difference between the normalized FRET ratio of cells without treatment and cells treated with 1 μM ($p < 0.0005$), and cells without treatment and cells treated with 2 μM cytochalasin B ($p < 0.0005$). At 24 h and 60 h, the FRET-derived glucose concentration was found to decrease with increasing dose of cytochalasin B (Fig. 8a). At 60 h, there was a significant difference between the glucose concentrations of cells treated with all doses of cytochalasin B (all $p < 0.05$). For the lactate reporter, immediately following addition of cytochalasin B, there was a significant difference between the normalized FRET ratio of cells treated with 1 μM and 4 μM ($p < 0.05$). At 60 h, there was a significant difference between the FRET-derived lactate concentration of cells without treatment and cells treated with 4 μM ($p < 0.01$), cells treated with 1 μM and 2 μM ($p < 0.05$), cells treated with 1 μM and 4 μM ($p < 0.0001$), and cells treated with 2 μM and 4 μM ($p < 0.01$). The maximum changes from untreated control cells were 0.4 ± 0.2 %, 0.9 ± 0.2 %, and 1.0 ± 0.3 % at baseline, 24 h, and 60 h (Fig. 8c).

Phloretin can function as an inhibitor of both GLUT and MCT4, the latter of which exports lactate. We imaged cells expressing the glucose or lactate FRET reporter over time to study the effect of phloretin on intracellular nutrient level. For the glucose reporter, immediately following addition of phloretin, there was a significant difference between the normalized FRET ratio of cells without treatment and cells treated with 20 μM ($p < 0.0005$), and cells treated with 10 μM and 20 μM phloretin ($p < 0.05$). At 24 h, there was a significant difference between the FRET-derived glucose concentration of cells without treatment and cells treated with 20 μM ($p < 0.0005$), and cells treated with 10 μM and 20 μM phloretin ($p < 0.05$). At 60 h, there were significant

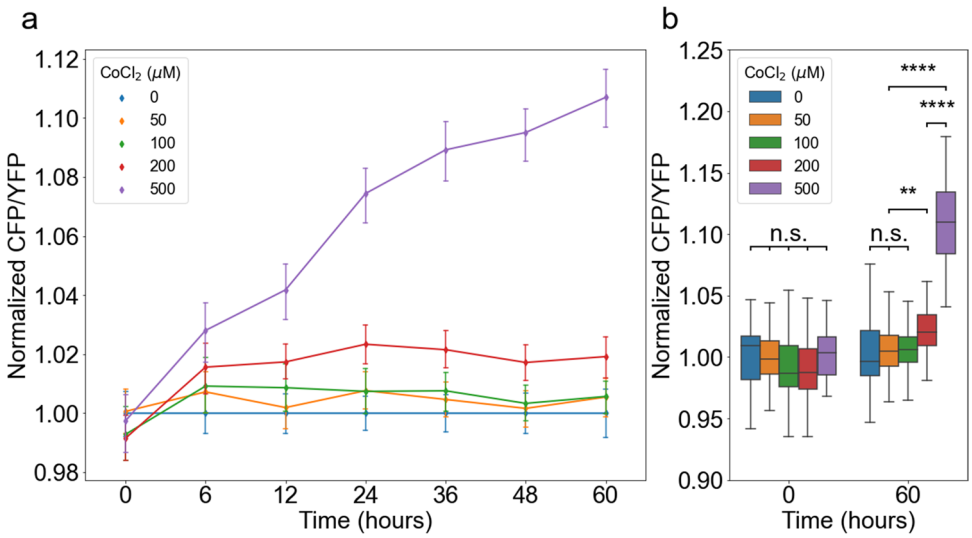

Fig. 7. Longitudinal FRET ratio of cells treated with $CoCl_2$. **a** shows the normalized FRET ratio for the lactate reporter in MDA-MB-231 cells treated with 0 μM, 50 μM, 100 μM, 200 μM, and 500 μM $CoCl_2$ over 60 h. Different colors represent different doses, with error bars calculated from 48 images of cells with the same dose. At each time point after baseline, the normalized FRET ratio increased with increasing $CoCl_2$ concentration. **b** displays boxplots of the normalized FRET ratio for cells treated with different $CoCl_2$ concentrations at 0 h and 60 h. Significance level is marked: n.s. = no significance; ** = $p < 0.01$; **** = $p < 0.0001$.

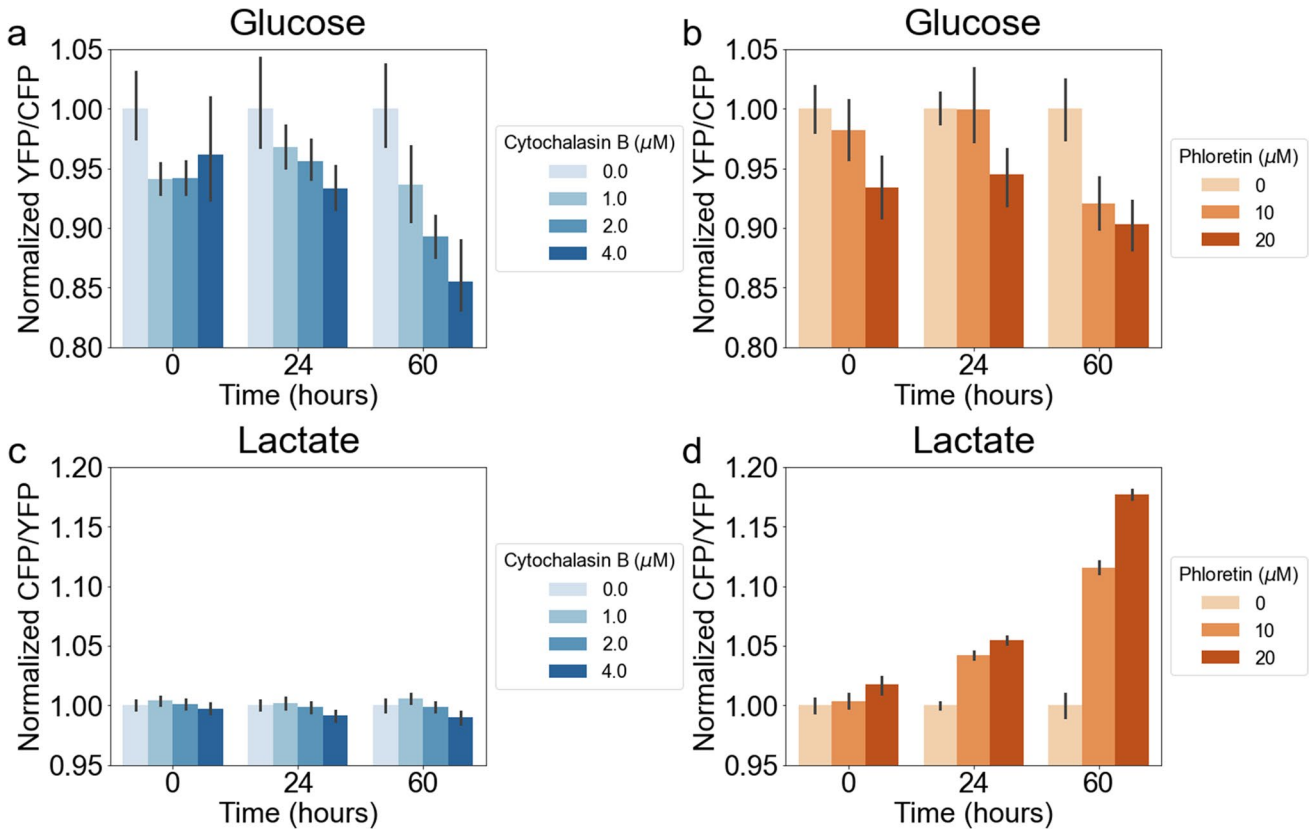

Fig. 8. FRET ratio of cells treated with glucose/lactate transporter inhibitors. **a** displays the normalized FRET ratio for the glucose reporter after 0, 24, and 60 h of treatment with cytochalasin B. **b** shows the normalized FRET ratio for the glucose reporter after 0, 24, and 60 h of treatment with phloretin. **c** displays the normalized FRET ratio for the lactate reporter after 0, 24, and 60 h of treatment with cytochalasin B. **d** shows the normalized FRET ratio for the lactate reporter after 0-, 24-, and 60-h treatment with phloretin. Different colors represented different doses. Error bar indicates the standard deviation of the normalized FRET ratio calculated from 48 images. Cells treated with cytochalasin B exhibited decreased glucose concentration but minimal decline in lactate concentration. Cells treated with phloretin exhibited decreased glucose concentration and increased lactate concentration.

differences between the normalized FRET ratio of cells without treatment and cells treated with 10 μM ($p < 0.0001$), and cells without treatment and cells treated with 20 μM phloretin (Fig. 8b; $p < 0.0001$). For the lactate reporter, immediately following addition of phloretin, there was a significant difference between normalized FRET ratio of cells without treatment and cells treated with 20 μM ($p < 0.0001$), and cells treated with 10 μM and 20 μM phloretin ($p < 0.005$). At 24 h and 60 h, there was a significant difference between the FRET-derived lactate concentration of cells treated with all doses of phloretin (all $p < 0.0001$). The maximum changes from untreated control cells were 1.8 ± 0.4 %, 5.5 ± 0.2 %, and 17.7 ± 0.2 % at baseline, 24 h, and 60 h (Fig. 8d).

Discussion

This study employed FRET reporters to assess intracellular glucose and lactate concentrations in a breast cancer cell line and monitor glucose and lactate dynamics. This approach can be used to elucidate the altered metabolism found in tumor cells. To accomplish this task, we stably transfected a glucose FRET reporter and lactate FRET reporter into a triple negative breast cancer cell line. We quantified the FRET ratio with both a confocal microscope and a live cell imaging plate reader and demonstrated correlation with ligand (glucose/lactate) concentration. We also performed longitudinal imaging to show that these reporters can noninvasively monitor changes induced by cellular metabolism. Finally, we used $CoCl_2$, cytochalasin B, and phloretin to perturb tumor cell metabolism and detected longitudinal changes in FRET reporters corresponding to metabolic inhibition.

Using a confocal microscope, the normalized FRET ratio was found to increase with increasing glucose concentration, demonstrating that intracellular glucose concentration can be measured via the FRET ratio. However this approach only imaged a small area of the cells and can be time-consuming to acquire a large quantity of images. Therefore, we used a live cell multi-mode reader for data acquisition for the remainder of this study. Using this system, we were able to acquire multiple images from a 96-well plate, allowing comparison of the FRET ratio with different ligand concentrations

supplied in the media. The positive correlation between the FRET ratio and the ligand concentration was confirmed for both glucose and lactate reporters. Using the plate reader with controlled temperature and CO_2, we performed longitudinal assessment of the glucose and lactate reporters. We found a positive correlation between FRET measurement and ligand concentration at each time point, meaning the ligand concentration–dependent FRET ratio response was robust and the FRET reporter could assay these ligands over time. For cells with glucose of 1 mM or higher, FRET measurements detected reduced glucose concentration over time, as tumor cells consumed glucose. The lack of significant correlation at lower glucose concentrations may stem from relatively smaller changes in the glucose concentration and suggests a limit in the sensitivity of this technique to detect small changes in glucose concentration. For cells plated in high lactate concentration media, we found a decline in the normalized FRET ratio over time. This putatively reflects utilization of lactate by tumor cells as extra nutrient resources. The FRET ratio showed different responses between low and high initial lactate concentrations, suggesting the reporters could be used as an indicator to detect metabolic switches.

The FRET reporters were used to examine the effect of several drugs intended to perturb intracellular nutrient levels. When cells were treated with $CoCl_2$ to induce hypoxia, a dose- and time-dependent increase in lactate was observed. Cytochalasin B, a GLUT1 inhibitor which inhibits glucose uptake, lowered glucose concentration in a dose- and time-dependent manner. Similarly, the cells treated with phloretin exhibited a lower normalized ratio for the glucose reporter compared to the control, reflecting blockage of the GLUT1 receptor. Additionally, phloretin led to higher measured lactate levels, reflecting the dual function of phloretin as it inhibited both glucose uptake and lactate export through MCT4. There were smaller, but significant, changes in the FRET ratio of the lactate reporter when cells were treated with cytochalasin B. This suggests alterations in intracellular lactate in response to GLUT1 blockage that may be investigated in future studies. The longitudinal nature of these studies provides insight into the dynamics of cytochalasin B and phloretin treatment. Both of these molecules induced changes in the FRET ratio at baseline, indicating that they have rapid activity. These studies of nutrient perturbation suggest that FRET reporters may be useful in developing other treatments that target cell metabolism by enabling longitudinal monitoring of treatment response. By comparing the relative change of glucose and lactate over time, we may be able to identify the potential target pathways and mechanisms for new drugs.

This work was performed in a single breast cancer cell line, but the results may be applicable across a range of cancer cells with similar metabolic pathways. Alternately, transfection of these FRET reporters in other cell lines may identify differences in metabolism between different cancers. For instance, GLUT1 is overexpressed in breast cancers [41] and MCT4 is expressed at a high level in MDA-MB-231 cells [42], but differences in these transporters across cell lines may lead to differential responses to therapy. While the work performed in this study was limited to *in vitro* studies, adoption of these tools for *in vivo* work is possible. Intravital imaging of these FRET reporters may permit *in vivo* imaging in preclinical cancer models [19, 30, 43]. Importantly, these *in vivo* studies would permit physiologically relevant monitoring of changes in metabolism, rather than requiring changes in cell media which do not fully reflect *in vivo* metabolism.

The present work develops an imaging platform for studying intracellular glucose and lactate concentrations with FRET reporters in a breast cancer cell line. This approach does not require an advanced imaging setup, specific buffering medium, or well-designed calibration. However, because of the simplistic design, we used a normalized FRET ratio to measure a relative change in glucose or lactate level in response to changes in ligand concentration or treatment. The reliable concentration ranges for the glucose FRET reporter and lactate FRET reporter are 0.05 to 9.6 mM [16] and 1 to 10 mM [17], respectively. While our current approach with plate-reader imaging could provide an easy and fast measurement to track the longitudinal change of glucose/lactate concentrations, it presented limited sensitivity at low ligand level, not taking the full advantage of these highly sensitive reporters. In addition, we assumed an equilibrium state of the nutrient concentration at each measurement point because of the relatively short measurement time (a few seconds for each image) compared to measurement interval (varying from 1 to 12 h) in our experiments. We also did not consider the kinetics of nutrient uptake and corresponding FRET ratio change in a short time scale (from seconds to minutes). We did not consider the effect of photobleaching, as the FRET reporter demonstrated insensitivity of the ratio to photobleaching [17]. The measurement and analysis of the FRET ratio should be further optimized to improve quantification of the glucose/lactate concentration. Factors that may affect the FRET response, such as other metabolites [17, 29] or pH [44], should be carefully examined and evaluated for their effect in the future.

Conclusions

We have established stable transfections of glucose and lactate reporters in a breast cancer cell line and demonstrated a ligand concentration–dependent FRET response over time. This system enables dynamic tracking of intracellular glucose and lactate in a triple negative breast cancer cell line. Using these FRET reporters, we detected dynamic changes in intracellular glucose and lactate concentrations in response to metabolism-directed therapies.

Author Contributions JY, TEY, JV, and HY contributed to the study design, analysis, data interpretation, and manuscript draft. JY, TD, AKS, YC, and

MJB contributed to data acquisition. All authors critically reviewed and approved the final version of the work.

Funding This project was supported by CPRIT for funding through RR160005 and RR160093, and the National Institutes of Health for funding through NCI U01CA174706, U01CA142565, and R01CA186193. T.E.Y is a CPRIT Scholar in Cancer Research. H.-C.Y. acknowledges the support from the Welch Foundation (F-1833), National Science Foundation (2029266) and National Institutes of Health (EY033106).

Declarations

Conflict of Interest The authors declare that they have no conflict of interest.

References

1. Forster J, Harriss-Phillips W, Douglass M, Bezak E (2017) A review of the development of tumor vasculature and its effects on the tumor microenvironment. HP Volume 5:21–32. https://doi.org/10.2147/HP.S133231
2. Hanahan D, Weinberg RA (2011) Hallmarks of cancer: the next generation. Cell 144:646–674. https://doi.org/10.1016/j.cell.2011.02.013
3. Warburg O (1956) On the Origin of Cancer Cells. Science 123:309–314
4. Vander Heiden MG, Cantley LC, Thompson CB (2009) Understanding the Warburg effect: the metabolic requirements of cell proliferation. Science 324:1029–1033. https://doi.org/10.1126/science.1160809
5. Cairns RA, Harris IS, Mak TW (2011) Regulation of cancer cell metabolism. Nat Rev Cancer 11:85
6. Pfeiffer T, Schuster S, Bonhoeffer S (2001) Cooperation and competition in the evolution of ATP-producing pathways. Science 292:504–507. https://doi.org/10.1126/science.1058079
7. Jose C, Bellance N, Rossignol R (2011) Choosing between glycolysis and oxidative phosphorylation: a tumor's dilemma?. Biochimica et Biophysica Acta (BBA) - Bioenergetics 1807:552–561. https://doi.org/10.1016/j.bbabio.2010.10.012
8. Gatenby RA, Gillies RJ (2007) Glycolysis in cancer: a potential target for therapy. Int J Biochem Cell Biol 39:1358–1366. https://doi.org/10.1016/j.biocel.2007.03.021
9. Gatenby RA, Smallbone K, Maini PK et al (2007) Cellular adaptations to hypoxia and acidosis during somatic evolution of breast cancer. Br J Cancer 97:646
10. Swietach P, Vaughan-Jones RD, Harris AL, Hulikova A (2014) The chemistry, physiology and pathology of pH in cancer. Phil Trans R Soc B 369:20130099. https://doi.org/10.1098/rstb.2013.0099
11. Corbet C, Feron O (2017) Tumour acidosis: from the passenger to the driver's seat. Nat Rev Cancer 17:577–593. https://doi.org/10.1038/nrc.2017.77
12. Som P, Atkins HL, Bandoypadhyay D et al (1980) A fluorinated glucose analog, 2-fluoro-2-deoxy-D-glucose (F-18): nontoxic tracer for rapid tumor detection. J Nucl Med 21:670–675
13. Zou C, Wang Y, Shen Z (2005) 2-NBDG as a fluorescent indicator for direct glucose uptake measurement. J Biochem Biophys Methods 64:207–215. https://doi.org/10.1016/j.jbbm.2005.08.001
14. Prodromidis MI, Karayannis MI (2002) Enzyme based amperometric biosensors for food analysis. 21
15. Rassaei L, Olthuis W, Tsujimura S et al (2014) Lactate biosensors: current status and outlook. Anal Bioanal Chem 406:123–137. https://doi.org/10.1007/s00216-013-7307-1
16. Takanaga H, Chaudhuri B, Frommer WB (2008) GLUT1 and GLUT9 as major contributors to glucose influx in HepG2 cells identified by a high sensitivity intramolecular FRET glucose sensor. Biochimica et Biophysica Acta (BBA) - Biomembranes 1778:1091–1099. https://doi.org/10.1016/j.bbamem.2007.11.015
17. Martın AS, Barros LF (2013) A genetically encoded FRET lactate sensor and its use to detect the Warburg effect in single cancer cells. PLoS ONE 8:11
18. Bittner CX (2010) High resolution measurement of the glycolytic rate. Front Neuroenerg 2. https://doi.org/10.3389/fnene.2010.00026
19. Sotelo-Hitschfeld T, Niemeyer MI, Machler P et al (2015) Channel-mediated lactate release by K+-stimulated astrocytes. J Neurosci 35:4168–4178. https://doi.org/10.1523/JNEUROSCI.5036-14.2015
20. Hasel P, Dando O, Jiwaji Z et al (2017) Neurons and neuronal activity control gene expression in astrocytes to regulate their development and metabolism. Nat Commun 8:15132. https://doi.org/10.1038/ncomms15132
21. Díaz-García CM, Mongeon R, Lahmann C et al (2017) Neuronal stimulation triggers neuronal glycolysis and not lactate uptake. Cell Metab 26:361-374.e4. https://doi.org/10.1016/j.cmet.2017.06.021
22. Vardjan N, Chowdhury HH, Horvat A et al (2018) Enhancement of astroglial aerobic glycolysis by extracellular lactate-mediated increase in cAMP. Front Mol Neurosci 11:148. https://doi.org/10.3389/fnmol.2018.00148
23. Jamali S, Klier M, Ames S et al (2015) Hypoxia-induced carbonic anhydrase IX facilitates lactate flux in human breast cancer cells by non-catalytic function. Sci Rep 5:13605. https://doi.org/10.1038/srep13605
24. Ames S, Pastorekova S, Becker HM (2018) The proteoglycan-like domain of carbonic anhydrase IX mediates non-catalytic facilitation of lactate transport in cancer cells. Oncotarget 9:27940–27957. https://doi.org/10.18632/oncotarget.25371
25. Ames S, Andring JT, McKenna R, Becker HM (2020) CAIX forms a transport metabolon with monocarboxylate transporters in human breast cancer cells. Oncogene 39:1710–1723. https://doi.org/10.1038/s41388-019-1098-6
26. Tobar N, Porras O, Smith PC et al (2017) Modulation of mammary stromal cell lactate dynamics by ambient glucose and epithelial factors: glucose modulates lactate transfer from stroma to epithelia. J Cell Physiol 232:136–144. https://doi.org/10.1002/jcp.25398
27. Ponce I, Garrido N, Tobar N, et al (2021) Matrix stiffness modulates metabolic interaction between human stromal and breast cancer cells to stimulate epithelial motility. In Review
28. Lucantoni F, Dussmann H, Prehn JHM (2018) Metabolic targeting of breast cancer cells with the 2-deoxy-D-glucose and the mitochondrial bioenergetics inhibitor MDIVI-1. Front Cell Dev Biol 6:113. https://doi.org/10.3389/fcell.2018.00113
29. Contreras-Baeza Y, Ceballo S, Arce-Molina R et al (2019) MitoToxy assay: a novel cell-based method for the assessment of metabolic toxicity in a multiwell plate format using a lactate FRET nanosensor. Laconic PLoS ONE 14:e0224527. https://doi.org/10.1371/journal.pone.0224527
30. Kondo H, Ratcliffe CDH, Hooper S et al (2021) Single-cell resolved imaging reveals intra-tumor heterogeneity in glycolysis, transitions between metabolic states, and their regulatory mechanisms. Cell Rep 34:108750. https://doi.org/10.1016/j.celrep.2021.108750
31. Dima AA, Elliott JT, Filliben JJ et al (2011) Comparison of segmentation algorithms for fluorescence microscopy images of cells: comparison of segmentation algorithms. Cytometry 79A:545–559. https://doi.org/10.1002/cyto.a.21079
32. Miller J (1991) Short report: reaction time analysis with outlier exclusion: bias varies with sample size. The Quarterly Journal of Experimental Psychology Section A 43:907–912. https://doi.org/10.1080/14640749108400962
33. Lee HR, Leslie F, Azarin SM (2018) A facile in vitro platform to study cancer cell dormancy under hypoxic microenvironments using CoCl2. J Biol Eng 12:12. https://doi.org/10.1186/s13036-018-0106-7
34. Macheda ML, Rogers S, Best JD (2005) Molecular and cellular regulation of glucose transporter (GLUT) proteins in cancer. J Cell Physiol 202:654–662. https://doi.org/10.1002/jcp.20166
35. Manel N, Kim FJ, Kinet S et al (2003) The ubiquitous glucose transporter GLUT-1 is a receptor for HTLV. Cell 115:449–459. https://doi.org/10.1016/S0092-8674(03)00881-X
36. Saab AS, Tzvetavona ID, Trevisiol A et al (2016) Oligodendroglial NMDA receptors regulate glucose import and axonal energy metabolism. Neuron 91:119–132. https://doi.org/10.1016/j.neuron.2016.05.016
37. Hu X, Chao M, Wu H (2017) Central role of lactate and proton in cancer cell resistance to glucose deprivation and its clinical translation. Sig Transduct Target Ther 2:16047. https://doi.org/10.1038/sigtrans.2016.47
38. Piasentin N, Milotti E, Chignola R (2020) The control of acidity in tumor cells: a biophysical model. Sci Rep 10:13613. https://doi.org/10.1038/s41598-020-70396-1
39. Granchi C, Minutolo F (2012) Anticancer agents that counteract tumor glycolysis. ChemMedChem 7:1318–1350. https://doi.org/10.1002/cmdc.201200176

40. Chen YI, Chang YJ, Liao SC et al (2020) Deep learning enables rapid and robust analysis of fluorescence lifetime imaging in photon-starved conditions. bioRxiv
41. Brown RS, Wahl RL (1993) Overexpression of glut-1 glucose transporter in human breast cancer an immunohistochemical study. Cancer 72:2979–2985. https://doi.org/10.1002/1097-0142(19931115)72:10%3c2979::AID-CNCR2820721020%3e3.0.CO;2-X
42. Gallagher SM, Castorino JJ, Wang D, Philp NJ (2007) Monocarboxylate transporter 4 regulates maturation and trafficking of CD147 to the plasma membrane in the metastatic breast cancer cell line MDA-MB-231. Can Res 67:4182–4189. https://doi.org/10.1158/0008-5472.CAN-06-3184
43. Mächler P, Wyss MT, Elsayed M et al (2016) In vivo evidence for a lactate gradient from astrocytes to neurons. Cell Metab 23:94–102. https://doi.org/10.1016/j.cmet.2015.10.010
44. Betolngar D-B, Erard M, Pasquier H et al (2015) pH sensitivity of FRET reporters based on cyan and yellow fluorescent proteins. Anal Bioanal Chem 407:4183–4193. https://doi.org/10.1007/s00216-015-8636-z